

## Studying Optical and Nonlinear Optical Properties of Synthesized Azo Dyes Doped in Polymer and Liquid Crystal Using Birefringence and Z-Scan Techniques

Nahid Hosain Nataj,<sup>1</sup> Ezeddin Mohajerani,<sup>1</sup> Hosein Nemati,<sup>1</sup> Alireza Moheghi,<sup>1</sup> Mohammad Reza Yazdanbakhsh,<sup>2</sup> Mohammad Goli,<sup>3</sup> Asadollah Mohammadi<sup>2</sup>

<sup>1</sup>Laser and Plasma Research Institute, Shahid Beheshti University G.C., Tehran, Iran

<sup>2</sup>Department of Chemistry, Faculty of Science, University of Guilan, Rasht, Iran

<sup>3</sup>Department of Chemistry, Shahid Beheshti University G.C., Tehran, Iran

Correspondence to: Dr. E. Mohajerani (E-mail: e-mohajerani@sbu.ac.ir)

**ABSTRACT:** The authors report the effect of the structure of new synthesized photo-responsive azo dyes, based on *N*-benzyl-*N*-ethyl-aniline on their optical and nonlinear optical properties, when doped in polymer and liquid crystal (LC) hosts. Anisotropic response of dyes doped with polymer polymethyl methacrylate is studied using photo-induced birefringence experiment and the optical nonlinearity of dyes doped in LC 5CB is measured using z-scan technique. A correlation is established between dipole moment and optical/nonlinear optical response, which makes it possible to develop molecular design strategies to create structures with suitable anisotropic response and nonlinearity in various host systems for different applications. It is also shown how very little change in the structure of the dye may cause severe changes in the dipole moment and its nonlinear response. © 2012 Wiley Periodicals, Inc. *J. Appl. Polym. Sci.* 000: 000–000, 2012

**KEYWORDS:** azo dye-doped polymer; birefringence; z-scan technique; anisotropic response; nonlinearity

Received 19 October 2011; accepted 18 March 2012; published online

DOI: 10.1002/app.37702

### INTRODUCTION

The azo dyes are by far the most important class, accounting for over 50% of all commercial dyes, and have been widely studied.<sup>1</sup> Amongst the azo dyes, heterocyclic diazo compounds have attracted much interest recently, especially those including sulfur and/or nitrogen.<sup>2–5</sup> In addition, host systems containing azo dyes have been developed for a wide range of photonic application such as reversible holographic data storage, image processing, and switching.<sup>6–9</sup> Examples of such systems are dye-doped polymers (DDP), dye-doped liquid crystals (DDLC), and dye-doped polymer dispersed liquid crystals (DDPDLC).<sup>10–12</sup> These compounds show well-known optical and nonlinear optical properties in resonant and nonresonant interaction of laser light such as anisotropic response by absorbing laser light, second harmonic generation, nonlinear refractive index, and electro optics in transparent region of the spectrum. On one hand, photo-induced birefringence in DDP is described as anisotropic response based on the *trans*–*cis*–*trans* reversible photoisomerization of azo chromophores followed by molecular re-orientation under the illumination of polarized light.<sup>13</sup> On the other hand,

coupled with liquid crystal (LC) molecules, the induced-birefringence due to the realignment of chromophores, greatly help the LC molecules to response to the laser-light field instead of electric field. When LCs are doped with dye agents, the dye-induced orientational effect, photoisomerization effect, and light-induced thermal effect come about to enhance LC nonlinearity.<sup>14–17</sup> In this case, z-scan technique is often used, which is a simple, yet powerful method for measuring nonlinear refractive indices (optical Kerr constant)  $n_2$  and absorption coefficients  $\alpha$ .

One of the most important parameters in photoresponse of azo dyes is the amount of induced anisotropy (or nonlinearity) and the other important parameter is the switching response time; depending on the application, one or both parameters could be emphasized. As it is known, anisotropic response and switching speed, depend on different parameters such as dye concentration, pump beam power, temperature, and especially, the structure of the chromophore. In our earlier study on azo dyes, the effect of different parameters such as sample thickness, concentration of dye in the polymer, and the laser pump power, on

© 2012 Wiley Periodicals, Inc.

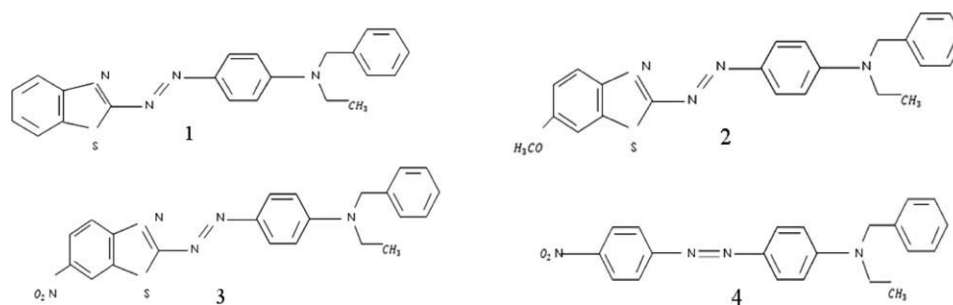


Figure 1. Structures of synthesized azo dyes 1, 2, 3, and 4.

the temperature dependence of the laser-induced birefringence in azo dye-doped polymer films was investigated. DR1-PMMA, DR13-PMMA, and MR-PMMA samples were studied and the optimized condition for obtaining the highest birefringence is achieved.<sup>10</sup> However, the need for synthesizing and characterizing new effective dyes and studying the effect of their structures on optical and nonlinear optical responses seems essential.

Chemical and optical characterization of seven synthesized azo dyes based on *N*-benzyl-*N*-ethyl-aniline is reported earlier.<sup>18</sup> In this article, four synthesized azo dyes based on their absorption peaks are chosen to study the effect of dye structure on the optical and nonlinear optical properties of azo dyes doped in polymer and LC hosts using birefringent and *z*-scan experiments. The effect of chemical functional groups added to the azo basis on optical and nonlinear optical response is explained. To interpret the results more precisely, a numerical evaluation of dipole moments is performed. The results are all interpreted using calculated dipole moment. It is shown that very little change in the structure of the dye may cause severe changes in the dipole moment and hence its nonlinear response.

## EXPERIMENTAL SECTION

### Materials and Sample Preparation

Figure 1 shows the molecular structures of four selected dyes synthesized in University of Guilan, Iran. The details of synthesis and characterization of those dyes are reported elsewhere.<sup>18</sup> Samples in form of thin layers of dyes doped polymethyl methacrylate (PMMA from Merck;  $m_p$ : 300°C, FW: 186.2,  $T_g$ : 125°C, inherent viscosity: 1.250) are prepared to study the birefringence of the samples induced by pump laser light. Samples are prepared by dissolving dye and polymer in common solvent (dichloromethane), to make a viscous solution suitable for dip coating. The samples are obtained from the solution by dip coating on clean glass substrate. Dyes 1, 2, 3, and 4 doped with PMMA are named DDP1, DDP2, DDP3, and DDP4, respectively. The concentration of polymer in the solvent is 0.1 g/mL and the concentration of all dyes in the polymer is 6%.<sup>10</sup> The thickness of all samples is 1.95  $\mu\text{m}$ . For *z*-scan experiment, nematic LC, 40-*n*-pentyl-4-cyanobiphenyl (5CB from Merck), is used as host. The LC is doped with the synthesized azo dyes. The ratio of the dye to the LC in all four mixtures is  $0.3 \pm 0.01\%$ . Standard cells (thickness 7.9  $\mu\text{m}$ , parallel alignments) are filled with the prepared mixtures by means of capillary action. In this article, dyes 1, 2, 3, and 4 doped with LC 5CB are named DDLC1, 2, 3, and 4, respectively.

### Observing the Spectrum of the Samples Before and During Laser Irradiation

Azo aromatic molecules are characterized spectroscopically by  $n-\pi^*$  and  $\pi-\pi^*$  bands in the electronic spectra. The differences between the *cis* and *trans* isomers are revealed by the amount of their absorbance. Thus, the *cis-trans*-isomerization of some azo groups can be monitored by intensity changes in the electronic spectra.<sup>19</sup> The UV-Vis absorption spectra of samples (Figure 2) are plotted before and during irradiation with 532 nm laser, to study the effect of irradiation on absorption peak of the samples. All experiments are performed in the dark room. The absorption peak during irradiation shows a reduction in height, which may be interpreted as a reduction in the *trans*-content due to the production of *cis*-isomers. Dye 3 shows very little changes in the absorption peak during laser irradiation. This might be due to its large-dipole moment, which reduces the isomerization yield and also possible relation between isomerization and peak wavelength. Note that the peak wavelength of this sample is very close to the wavelength of the pump laser light and also the absorption of this sample is much higher than other samples.

### Experiments

**Photo-Induced Birefringence.** Figure 3 shows the experimental setup used to measure photo-induced birefringence. To study the photo-induced birefringence of the DDPs as a function of time, a CW-second harmonic Nd:YAG laser (wavelength 532 nm, power 6 mw) is switched on and off as pump beam and a He-Ne Laser (wavelength 633 nm, power < 2 mw) is used as probe beam to monitor the changes in the refractive index. A pair of crosspolarizers at 45° to the polarization direction of the pump beam is used to monitor the induced retardation due to changes in the refractive index. A photodetector detects the transmitted-light intensity of the probe beam after passing through the crosspolarizers as a measure of induced birefringence. All experiments are performed at room temperature under ambient condition.

**Z-scan Technique.** The experimental setup for evaluating both the linear absorption and *z*-scan of DDLC samples is depicted in Figure 4. The experiment is performed with a second-harmonic CW laser Nd:YAG (532 nm). The director of LC molecules is aligned parallel to the direction of the polarization of the laser beam. In addition, the authors used a beam splitter and a photodetector in a reference arm to ensure that the laser power remains constant during the experiment. A lens ( $f = 15$

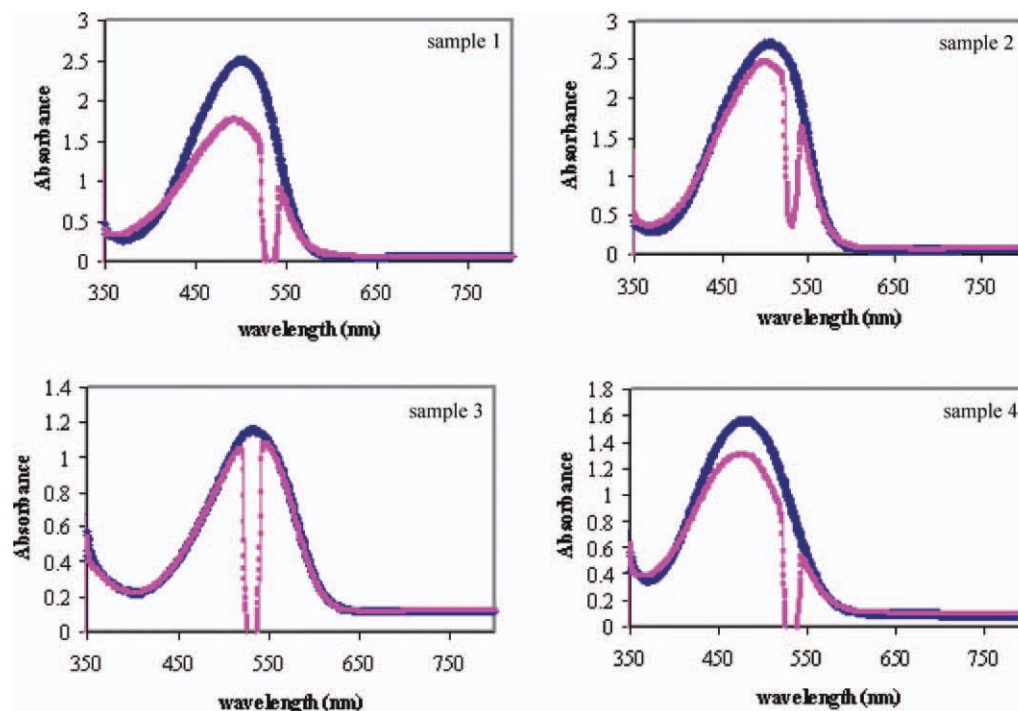


**Figure 2.** UV-visible spectra of thin films of azo dyes 1, 2, 3, and 4 doped PMMA. In each figure, the upper and lower curves are related to spectrum before and during irradiation of 532 nm laser beam. [Color figure can be viewed in the online issue, which is available at [wileyonlinelibrary.com](http://wileyonlinelibrary.com).]

cm) focuses the light on the samples. An iris was put in front of another photodetector to limit the transmitted light to have a large signal to noise ratio.<sup>17</sup> The iris is adjusted to pass 40% of overall power. All experiments are performed at room temperature.

## RESULTS AND DISCUSSION

### Dipole Moment Calculation

Since the electric-dipole moments of the heterocyclic azo dyes were not available experimentally, they were computed using computational density functional based methods. Using Gaussian program,<sup>20</sup> in the first step, the most stable conformers of each molecule were determined from an automatic conformational search by MM2 force field<sup>21</sup> as a fast molecular mechanics method and then, the most stable conformers were re-optimized at B3LYP/6-31g(d)<sup>22,23</sup> level of theory. The frequencies of the normal mode of the optimized geometries were calculated and it was demonstrated that all optimized structures are true

local minima (no imaginary frequencies were observed). Subsequently, the most stable conformer of each molecule was re-optimized at B3LYP/6-311 + g(d) level<sup>22,24</sup> (Figure 5) and the electric-dipole moments were calculated for each conformer. The calculated-dipole moments of heterocyclic azo dyes 1, 2, and 3 are 5.7, 5.0, and 13.4 Debye, respectively. The value of dipole moment of azobenzene dye 4 is 10.9 Debye. The amount of dipole moment for this azobenzene compound is found to be close to the reported value for this class of dyes.<sup>25</sup> The lower amount of dipole moment of the heterocyclic azo dyes 1 and 2 in comparison with azobenzene type dye 4 could be related to their lower push-pull character and asymmetric position of acceptor and donor groups. The highest push-pull character, within the set of compounds shown in Figure 1, is presented in dye 3 and dye 4. The synthesized dye 3 has strong acceptor NO<sub>2</sub>, which seems to impose great asymmetric functional groups position. Therefore, it has the highest push-pull character among four dyes, and hence the highest amount of dipole

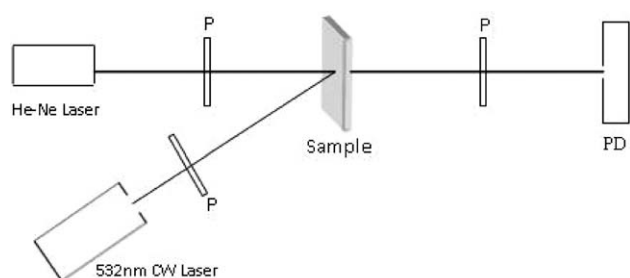


**Figure 3.** Experimental setup for birefringence experiment; P: polarizer, PD: photo detector.

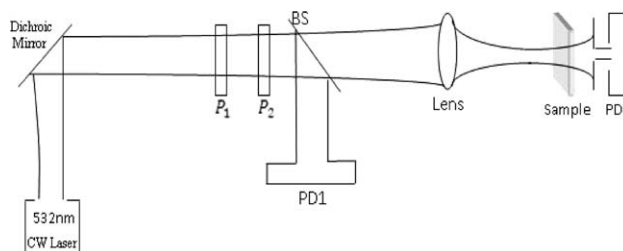


**Figure 4.** Experimental arrangement for measuring the linear absorption and z-scan technique; P: polarizer, PD: photo detector, BS: beam splitter.

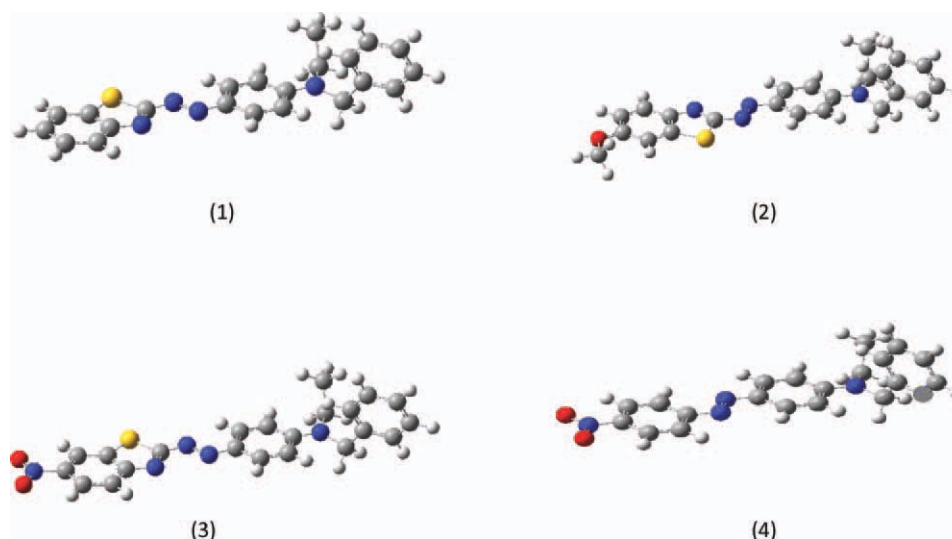


**Figure 5.** The three-dimensional optimized structure of the most stable conformers of each sample (compare with Figure 1 for numbers). The gray spheres are carbon atoms, yellow spheres display sulfur atoms, blue spheres are nitrogen atoms, red spheres are oxygen atoms, and the white small spheres display the hydrogen atoms of each conformer. [Color figure can be viewed in the online issue, which is available at [wileyonlinelibrary.com](http://wileyonlinelibrary.com).]

moment. It will be shown that this enhancement in the dipole moment of dye 3 affects its nonlinear responses drastically.

#### Effect of Chromophore Structure on the Photo-induced Birefringence

The transmitted intensity of the probe He–Ne laser (as a measure of birefringence) of DDP1 to DDP4 samples shows a sharp increase and then reaches its maximum value (i.e., saturation) slowly. The transmitted intensity after reaching to the saturation is presented in Table I. Figure 6 shows the transmitted intensity of probe He–Ne beam versus dipole moment of DDP1–DDP4 samples. The amount of dipole moment of DR1 and DR13<sup>25</sup> and their corresponding measured transmitted intensity<sup>26</sup> is also shown in Figure 6 for better comparison. DDP1 and DDP2 have a benzothiazole and *N*-benzyl-*N*-ethyl-aniline as a strong acceptor and coupling component, respectively (Figure 1). They differ only by a donor group (OCH<sub>3</sub>) attached to benzothiazole ring in the dye structure of DDP2, which reduces the dipole moment as presented in Section “Dipole Moment Calculation.” The OCH<sub>3</sub> group in DDP2 also causes more push–pull character and charge transfer due to an additional resonance between methoxy and thiazole ring, which leads to higher isomerization yield. Larger amount of photo-induced birefringence in this sample is also due to more molecular reorientation due to *cis*–*trans*-isomerization. DDP3 has also a heterocyclic azo dye, which differs from DDP2 by substituting the donor OCH<sub>3</sub> by a strong acceptor NO<sub>2</sub>. The unusual slow increase in the birefringence of DDP3 seems to be related to its large dipole moment and hence little isomerization yield when compared with other known azo chromophores.<sup>25</sup> The photo-induced response of DR1 and DR13 is in good agreement with the above discussion, as shown in Figure 6. In the *z*-scan experiments, it will be shown that DDLC3, which contains dye3, saturates much faster which may be related to larger life time of the *cis* isomer when compared with other samples, which are all due to its large amount of the dipole moment. DDP4 has an azo-benzene

compound with a different structure. The authors studied azo benzene compound for comparing with heterocyclic azo dyes. It is known that heterocyclic dyes show more bathochromic shift when compared with azo benzene dyes. Table I also shows that the amount of birefringence in DDP4 is less than that of DDP1 and DDP2, which could be related to its larger dipole moment.

To study the mechanisms involved in the photo-induced anisotropy in DDP1, 2, and 4 more precisely, the experimental growth and decay curves of birefringence<sup>18</sup> are fitted with the best-possible functions.<sup>6,10</sup> Note that the authors exclude sample 3 because of its unusual behavior. For growth of birefringence after switching the pump on, the biexponential function [eq. (1)] is used, in which *a* and *c* are constants.  $\tau_f$  and  $\tau_s$  are fast and slow time constants. Fit parameters are listed in Table II.

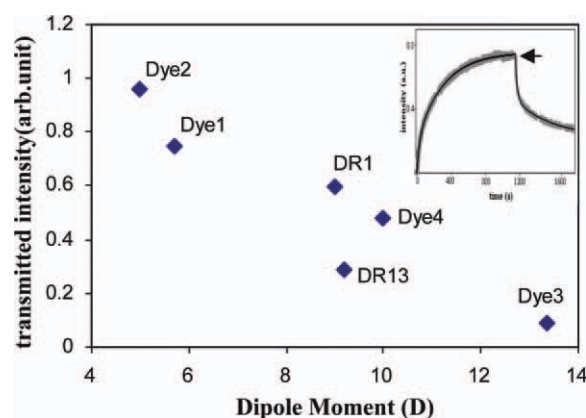


**Figure 6.** Transmitted intensity due to photo-induced birefringence versus dipole moment for DR1, DR13, and DDP1–DDP4. The inset exhibits the photo-induced birefringence of DDP1 as an example. The flash shows the reported transmitted intensity as a measure of birefringence. [Color figure can be viewed in the online issue, which is available at [wileyonlinelibrary.com](http://wileyonlinelibrary.com).]



**Table I.** The Experimental Data Obtained From Absorption Spectroscopy, Dipole Moment Calculation, Birefringence, and Z-scan Experiments

	Dye 1	Dye 2	Dye 3	Dye 4
Peak $\lambda$ (nm)	500	505	536	481
Linear absorbance ( $\text{cm}^{-1}$ ) DDLC1-4	0.06	0.08	0.22	0.09
Dipole moment (D)	5.7	5	13.4	10
Transmitted intensity due to birefringence for DDP1-4 (AU)	0.75	0.96	0.09	0.48
$N_2$ ( $\text{cm}^2/\text{w}$ ) $\times 10^{-5}$ dye-doped LC	4.835	4.839	N/A	3.643

$$\Delta I = a[1 - \exp(-t/\tau_f)] + c[1 - \exp(-t/\tau_s)] \quad (1)$$

By turning the pump beam on, the initial fast anisotropic response of the samples is due to the *trans-cis*-photoisomerization (characterized by fast time constant), and then slow reorientation, caused by angular orientation of *cis*-isomers followed by transformation to the *trans* state (characterized by slow time constant).

Due to more push-pull effect and smaller dipole moment, the fast process in DDP2 is larger in importance (“*a*” constant in the function) than that of DDP1 and also the *trans-cis-trans* photoisomerization and following reorientation in DDP2 will occur more slowly, as is evident in fast and slow time constants. Dye 4 as an azo benzene chromophore has largest dipole moment value and slowest response time in comparison to dyes 1 and 2.

In relaxation of birefringence, upon termination of pump beam, there is not any further photoisomerization and the behavior of the samples is to some extent similar. For all three samples, the dynamics may be fitted using a decay function [eq. (2)] with two terms.

$$\Delta I = a \exp[-(t - t_0)/\tau_f] + c \exp[-(t - t_0)/\tau_s] \quad (2)$$

By turning the pump beam off, the remaining *cis*-isomers transform to *trans*. Also in relaxation process, the *trans*-isomers, which preferred to align perpendicular to the electric field of light, will relax and the sample lose its anisotropy. Therefore, the decay process occurs again in two steps: fast thermal *cis-to-trans* isomerization (fast decay time constant) and the angular diffusion of *trans*-isomers (slow time constant in decay function). Although the rate of losing alignment after turning the pump off is fastest for DDP4, the fast part of the decay, which is related to the life time and the population of the *cis*-isomer, is almost similar for all three samples (Table III). It had to be noted that also the amount of birefringence is higher in our

**Table II.** Parameters Obtained by Fitting the Birefringence Build-up Data

Sample	A	$\tau_f$ (s)	c	$\tau_s$ (s)	$R^2$ (regression)
DDP1	0.224	28.7	0.568	303	0.9984
DDP2	0.663	50.5	0.416	526.3	0.9979
DDP4	0.203	52.9	0.300	277.8	0.9963

new synthesized dyes, the build up, and decay response times of all dyes are slower than that of Disperse Red1 (DR1), Disperse Red13 (DR13), and Methyl Red (MR), which is reported in.<sup>10,26</sup>

### Z-scan Experiments on Azo Dye-Doped LC Films

Linear absorption of the DDLCs is an important parameter to evaluate the nonlinear refractive index of these samples due to the mechanism involved in light-induced alignment of DDLC.<sup>14-16</sup> From Figure 7, it is seen that the linear absorption of the DDLCs increases linearly by increasing the incident power, as it is expected. The absorption coefficient ( $\alpha$ ), which is calculated by Beer-Lambert equation for each of four dyes, is presented in Table I. A closed aperture scheme allowed us to determine both the sign and the value of the nonlinear refractive index. As shown in Figure 8, in all samples except DDLC3, a peak is followed by a valley, which states that the samples have negative optical nonlinear indices, known as self-defocusing.<sup>17</sup> Such nonlinearity is due to photoisomerization and reorientation of azo dyes and the following LC molecular reorientation. As well explained in Ref. 27 for a Gaussian laser beam, the LC director in the central region of the illuminated spot tends to be re-oriented at a larger angle from the direction of polarization of the laser than the directors of the LCs in the outer region. Therefore, the pump beam encounters with a smaller refractive index in the central region than in the outer region, causing self-defocusing. The thermal effect also contributes to this nonlinearity. When azo dyes absorb laser light, the heat released from photoisomerization increases the temperature of the DDLC film. The thermal effect presents a smaller refractive index in the central region of the illuminated spot than in the outer region as determined by the temperature-dependent refractive index of the nematic LC. This effect is also defocusing.

The authors calculated the parameters  $\Delta\phi_0$ , phase shift of the center of the beam propagated through the sample,  $\Delta T_{p-v}$ , the peak to valley change in the transmittance and  $n_2$ , optical nonlinear refractive index using the empirical eq. (3 and 4) extracted from Ref. 17 The beam radius at waist and the

**Table III.** Parameters Obtained by Fitting the Birefringence Decay Data

Sample	A	$\tau_f$ (s)	c	$\tau_s$ (s)	$R^2$
DDP1	0.2641	19.27	0.2136	344.8	0.9896
DDP2	0.2541	19.84	0.2482	277.8	0.9930
DDP4	0.1881	17.24	0.1366	212.8	0.9845

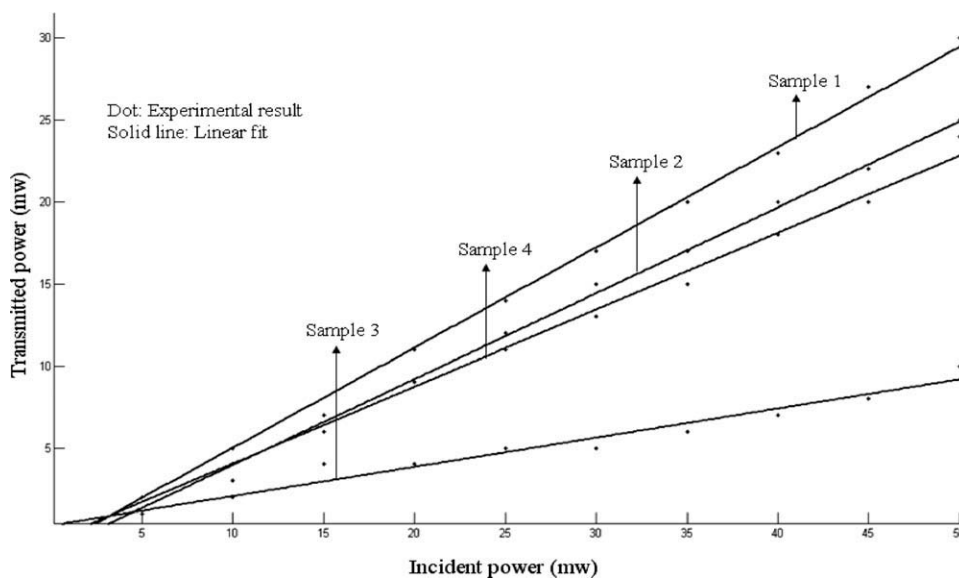


Figure 7. Linear behavior of the absorption effect in the low power regime of DDLCs 1–4.

Rayleigh parameter are 90  $\mu\text{m}$  and 48 mm, respectively, and incident power intensity is 70 mw.

$$\Delta\phi_0 = \frac{2\pi L_{\text{eff}} n_2 I}{\lambda} \quad (3)$$

$$\Delta T_{p-v} = 0.406(1 - S)^{0.27} \Delta\phi_0 \quad (4)$$

Where  $L_{\text{eff}} = \frac{1 - \exp(-\alpha L)}{\alpha}$ , and  $S$  is the power fraction transmitted by the aperture.

The amount of  $\Delta\phi_0$  for samples 1, 2, and 4 is 1.237, 1.238, and 0.932, respectively.  $\Delta T_{p-v}$  of samples 1, 2, and 4 is obtained 0.437, 0.438, and 0.330, respectively. Again in these experiments, as presented in Table I, samples 1 and 2, which contains heterocyclic dyes, show stronger optical nonlinearity than that of sample 4, which is azo benzene. As shown in Table I, the absorption peak of synthesized dye 3 is very close to the pump wavelength (532 nm green laser), which has the largest amount of dipole

moment and linear absorbance coefficient. In addition, the z-scan experiment result shows a behavior similar to open aperture situation, which is due to its large absorbance and rapid saturation. Finally, the consistence of the results of both experiments confirms the role of dipole moment and push-pull effect in the chromophore.

## CONCLUSION

The authors have observed the polarized-light induced anisotropy in polymer and LC films-doped with synthesized azo dyes using photo-induced birefringence and z-scan experiments. The structure of azo dyes and their functional groups has significant role on their induced anisotropy and response time. By comparing synthesized azobenzene dye 4 and other commercially available dyes such as DR1 and DR13, with heterocyclic azo dyes such as dyes 1 and 2, it is clear that heterocyclic azo dyes shows greater anisotropic response. However, the response times of heterocyclic dyes 1 and 2 are greater than that of azobenzene dyes. Interestingly, the heterocyclic azo dye 3 showed very slow and small anisotropic behaviors and large linear absorption, which could be related to its large-dipole moment as a result of strong acceptor  $\text{NO}_2$  and asymmetric group position. In fact, its large-dipole moment causes low isomerization yield and long *cis* life time, which ends with its unusual optical response to the polarized light.

These results allow one to draw some correlation between the molecular structure and the anisotropic response and nonlinearity, designing organic compounds with high birefringence, great nonlinearity, and proper response time in various host systems and for different applications.

## ACKNOWLEDGMENTS

The authors would like to thank Dr. Shahbazian, Dr. Bazgir, Dr. Shahrousvand, and Dr. Nourmohammadian for valuable discussions.

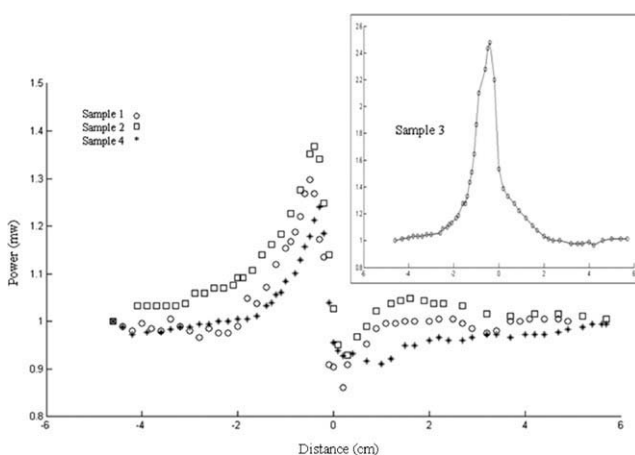


Figure 8. Normalized closed aperture z-scan experimental curves of DDLC1, 2 and 4. The inlet exhibits the unusual behavior of DDLC3

## REFERENCES

1. Hunger, K. *Industrial Dyes. Chemistry, Properties and Applications*, 3rd ed.; Wiley-VCH, Weinheim, **2003**.
2. Matsui, M.; Kamino, Y.; Hayashi, M.; Funabiki, K.; Shibata, K.; Muramatsu, H.; Abe, Y.; Kaneko, M. *Liquid Crystals*, **1998**, *25*, 235.
3. Moylan, C. R.; Twieg, R. J.; Lee, V. Y.; Swanson, S. A.; Betterton, K. M.; Miller, R. D. *J. Am. Chem. Soc.*, **1993**, *115*, 12599.
4. Samyn, C.; Verbiest, T.; Kesters, E.; Van den Broeck, K.; Van Beylen, M.; Persoons, A. *Polymer*, **2000**, *41*, 6049.
5. Bruno, V.; Castaldo, A.; Centore, R.; Sirigu, A.; Sarcinelli, F.; Casalboni, M.; Pizzoferrato, R. *J. Polym. Sci. A Polym. Chem.*, **2002**, *40*, 1468.
6. Natansohn, A.; Rochon, P. *Chem. Rev.*, **2002**, *102*, 4139.
7. Ono, H.; Kowatari, N.; Kawatsuki, N. *Opt. Mat.*, **2001**, *17*, 387.
8. Nemati, H.; Mohajerani, E.; Moheghi, A.; Behzadi Rad, M.; Hosain Nataj, N. *EPL*, **2009**, *87*, 64001.
9. Si, J.; Mitsuyu, T.; Ye, P.; Shen, Y.; Hirao, K. *Appl. Phys. Lett.*, **1998**, *72*, 762.
10. Mohajerani, E.; Hosain Nataj, N. *Opt. Mat.*, **2007**, *29*, 1408.
11. Fuh, A. Y.; Lee, C.; Mo, T. J. *Opt. Soc. Am. B*, **2002**, *19*, 2590.
12. Matsui, T.; Ozaki, M.; Yoshino, K. *J. Opt. Soc. Am. B*, **2004**, *21*, 1651.
13. Yang, J.; Zhang, J.; Liu, J.; Wang, P.; Ma, H.; Ming, H.; Li, Z.; Zhang, Q. *Opt. Mat.*, **2004**, *27*, 527.
14. Lin, H. C.; Fuh, A. Y. *J. Nonlinear Opt. Phys. Mat.*, **2009**, *18*, 367.
15. Jánossy, I.; Lloyd, A. D.; Wherrett, B. S. *J. Mol. Cryst. Liq. Cryst.*, **1990**, *179*, 1.
16. Mousavi, S. H.; Majles Ara, M. H.; Soheilian, F.; Koushki, E.; Salmani, S.; Bahramian, R. *J. Mol. Cryst. Liq. Cryst.*, **2008**, *488*, 23.
17. Sheik Bahae, M.; Said, A. A.; Van Styland, E. W. *Opt. Lett.*, **1989**, *14*, 955.
18. Yazdanbakhsh, M. R.; Mohammadi, A.; Mohajerani, E.; Nemati, H.; Hosain Nataj, N.; Moheghi, A.; Naemikhah, E. *Mol. Liq.*, **2010**, *151*, 107.
19. Xie, S.; Natansohn, A.; Rochoni, P. *Chem. Mater.*, **1993**, *5*, 403.
20. Frisch, M. J.; Trucks, G. W.; Schlegel, H. B.; Scuseria, G. E.; Robb, M. A.; Cheeseman, J. R.; Zakrzewski, V. G.; Montgomery, J. A., Jr.; Stratmann, R. E.; Burant, J. C.; Dapprich, S.; Millam, J. M.; Daniels, A. D.; Kudin, K. N.; Strain, M. C.; Farkas, O.; Tomasi, J.; Barone, V.; Cossi, M.; Cammi, R.; Mennucci, B.; Pomelli, C.; Adamo, C.; Clifford, S.; Ochterski, J.; Petersson, G. A.; Ayala, P. Y.; Cui, Q.; Morokuma, K.; Malick, D. K.; Rabuck, A. D.; Raghavachari, K.; Foresman, J. B.; Cioslowski, J.; Ortiz, J. V.; Baboul, A. G.; Stefanov, B. B.; Liu, G.; Liashenko, A.; Piskorz, P.; Komaromi, I.; Gomperts, R.; Martin, R. L.; Fox, D. J.; Keith, T.; Al-Laham, M. A.; Peng, C. Y.; Nanayakkara, A.; Challacombe, M.; Gill, P. M. W.; Johnson, B.; Chen, W.; Wong, M. W.; Andres, J. L.; Gonzalez, C.; Head-Gordon, M.; Replogle, E. S.; Pople, J. A.; Gaussian 98; Revision A.9; Gaussian: Pittsburgh PA, **1998**.
21. Allinger, N. A. *J. Am. Chem. Soc.*, **1977**, *99*, 8127.
22. Becke, A. D. *J. Chem. Phys.*, **1993**, *98*, 5648.
23. Hariharan, P. C.; Pople, J. A. *Theor. Chem. Acta*, **1973**, *28*, 213.
24. Raghavachari, K.; Trucks, G. W. *J. Chem. Phys.*, **1989**, *91*, 1062.
25. De Boni, L.; Rodrigues, J. J., Jr.; dos Santos, D. S., Jr.; CSilva, H.T. P.; Balogh, D. T.; Oliveira, O. N., Jr.; Zilio, S. C.; Misoguti, L.; Mendonca, C. R. *Chem. Phys. Lett.*, **2002**, *361*, 209.
26. Mohajerani, E.; Hosain Nataj, N. *Opt. Mat.*, **2007**, *29*, 1408.
27. Lin, H. C.; Chen, C. H.; Mo, T. S.; Li, M. S.; Lee, C. R.; Hsieh, F. M.; Liu, J. H.; Fuh, A. Y. *J. Opt. Com.*, **2010**, *283*, 323.